Available online at www.sciencedirect.com
SCIENCE DIRECT®
International Journal of Pharmaceutics 275 (2004) 19–27
international journal of pharmaceutics
www.elsevier.com/locate/ijpharm

Influence of physicochemical properties and intestinal region on the absorption of 3-fluoro-2-pyrimidylmethyl 3-(2,2-difluoro-2-(2-pyridyl)ethylamino)-6-chloropyrazin-2-one-1-acetamide, a water insoluble thrombin inhibitor, in dogs

Danielle Euler, Patricia Frech, Shyam Karki, Cameron Cowden, Gareth Pearce, Pratik Mehta, Christopher Lindemann, Paul Byway, Michael Wang, Todd Gibson, Yu Cheng, Gloria Kwei, Jayna Rose*

Department of Pharmaceutical Research and Development, Merck & Co., Inc., West Point, PA 19486, USA

Received 17 September 2003; received in revised form 16 December 2003; accepted 22 December 2003

Abstract

In this paper, we describe the physicochemical and biopharmaceutical properties of 3-fluoro-2-pyrimidylmethyl 3-(2,2-difluoro-2-(2-pyridyl)ethylamino)-6-chloropyrazin-2-one-1-acetamide, a direct thrombin inhibitor (**1**, Fig. 1). Three crystalline forms were characterized and studies were planned to investigate the absorption characteristics of the three selected crystalline forms. Due to the short half-life observed in preclinical species, regional absorption studies were also conducted to support potential controlled release formulation development. Results showed that the absorption of **1** was dependent on the surface area of the particles administered as suspensions and was independent of the crystal forms. From Caco-2 cell transport studies, it was determined that the permeability of **1** was high. Based on the low aqueous solubility it would be classified as a class 2 compound in the Biopharmaceutics Classification System. Regional absorption results suggested that the compound was absorbed along the gastrointestinal tract in Beagle dogs, however colonic absorption appeared to be reduced by slower dissolution.

Keywords: Surface area; Polymorphism; Intestinal absorption

1. Introduction

The standard treatment for DVT includes an initial course of heparin or low-molecular weight heparin in combination with coumarins, followed by long-term treatment with coumarins alone. Each agent has its disadvantages. Heparin must be administered parenterally. Coumarins have a narrow therapeutic index, display a slow onset of action and have the potential for drug/food interactions. Frequent coagulation monitoring is necessary to avoid bleeding caused by overtreatment or a risk of thrombosis caused by undertreatment (Gustafsson et al., 2001; Wahlander et al., 2002). These limitations have stimulated the development of new anticoagulant therapies including direct thrombin inhibitors.

There is a need for new therapeutic agents for the chronic treatment of DVT. Ideally these agents would display a wide safety margin and appropriate

* Corresponding author. Tel.: +1-215-652-0051.

0378-5173/$ – see front matter © 2004 Elsevier B.V. All rights reserved.
doi:10.1016/j.ijpharm.2003.12.021

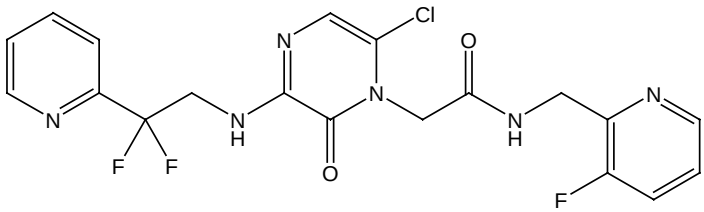

Fig. 1. Structure of **1**: 3-fluoro-2-pyrimidylmethyl 3-(2,2-difluoro-2-(2-pyridyl)ethylamino)-6-chloropyrazin-2-one-1-acetamide.

physicochemical and pharmacokinetic properties permitting oral dosing. In this paper, we describe the physicochemical and biopharmaceutical properties of a direct thrombin inhibitor (**1**) which has been previously described in the literature (Burgey et al., 2003). Three crystalline forms of **1** were characterized and studies were planned to investigate the absorption characteristics of these forms. Due to the short half-life observed in preclinical species, regional absorption studies were also conducted to support potential controlled release formulation development.

2. Materials

3-Fluoro-2-pyrimidylmethyl 3-(2,2-difluoro-2-(2-pyridyl)ethylamino)-6-chloropyrazin-2-one-1-acetamide (Fig. 1) was obtained from the Process Research Department, Merck Research Laboratories, Hoddesdon, England. Methylcellulose, hydroxypropylcellulose, sodium lauryl sulfate, hydroxypropyl-β-cyclodextrin and Hanks buffered saline solution (HBSS) were commercially available.

3. Methods

3.1. Physicochemical characterization

The identification of polymorphs and hydrates was determined by X-ray powder diffraction (XRPD), differential scanning calorimetry (DSC) and thermogravimetric analysis (TGA). The XRPD patterns were recorded at a scanning speed of 0.020°/s with a scanning angle of 4–40° 2-theta, a voltage of 50 kV, and a current of 40 mA (model D5000 Diffraktometer, Siemens). DSC analysis was conducted as a modulated mode scanning under nitrogen flow at a heating rate of 10 °C/min (model 2920 modulated DSC, TA Instruments). The TGA analysis was conducted under nitrogen flow at a heating rate of 10 °C/min (model 2050, TA Instruments).

The surface area was determined by the BET method (Quantachrome NOVA 1200) with nitrogen as the adsorbate gas. The particle size was determined by optical microscopy or laser scattering sizing (Microtrac). Scanning electron microscopy was conducted using a Philips Electro Scan ESEM 2020. Micrographs were collected at ambient temperature with an operating voltage of 20 kV and a filament current of 1.81 mA at 5 Torr for image acquisition. The micrographs were acquired over a 30 s time period.

3.2. In vivo studies

All procedures were approved by the Merck Research Laboratories Institutional Animal Care and Use Committee and all research adhered to the “Guide for the Care and Use of Laboratory Animals” (Institute of Laboratory Animal Resources, National Research Council, revised in 1996).

3.2.1. Animal experiments

Male Beagle dogs were obtained from Marshall Farms (North Rose, NY) and housed in a USDA-approved facility according to AAALAC guidelines. Chronic vascular access ports were surgically implanted under anesthesia in some dogs several weeks before dosing. The animals were used in a randomized crossover design. The animals were fasted up to 16 h before each study period. Water was returned at 2 h and food was returned at 4 h post dosing. The suspension or solution was administered via oral gavage or intestinal cannulae. Blood samples were removed from cephalic vein catheters for the

first eight hours post dosing. Blood samples at later time points were taken by venipuncture. Blood samples were taken prior to dosing and at 15 min, 30 min, 1, 2, 3, 4, 6, 8, 12, and 24 h after dosing. Plasma was separated by centrifugation (4 °C, 2500 rpm, 15 min) and kept frozen (−70 °C) until analysis by LC/MS/MS.

3.2.2. Preparation of dosing suspensions and solutions

Aqueous suspensions of **1** were prepared on the day of each study with a mortar and pestle using 0.5% methylcellulose or 1.25% hydroxypropylcellulose (HPC-SL) as the suspending agent at concentrations of 0.2, 10 and 20 mg/ml. An acidified aqueous solution of the thrombin inhibitor **1** was prepared at a concentration of 10 mg/ml. The final pH of the solution was 1.0. For the regional absorption studies, a solution of **1** was prepared with 50% hydroxypropyl-β-cyclodextrin (HPβCD).

A colloidal dispersion formulation was prepared with the monohydrate A form of **1** using methods described in the literature (Merisko-Liversidge et al., 2003). The nanoparticles were prepared with the NanoMill® milling system (Elan Drug Delivery, King of Prussia, PA) using Polymill 500 (polystyrene beads) as the grinding media. Hydroxypropylcellulose (HPC-SL) and sodium lauryl sulfate (SLS) were used as the stabilizers. The final dispersion contained 12% TI, 2% HPC-SL and 0.12% SLS. The rotation speed of the NanoMill® milling system was 5000 rpm. Particle size was measured after dosing using a Horiba LA 910 with a relative refractive index of 1.2 ± 0.00 i. The mean particle size was approximately 0.170 μm.

The particle size of the anhydrous A form of **1** was optimized with the Nektar supercritical fluid technology (SCF) using a process described in the literature (Palakodaty and York, 1999; Edwards et al., 2001). The surface area of the final needle-like crystalline material was 35 m^2/g, measured with the Horiba Surface Area Analyzer SA-6200 and the morphology of the particles remained the same as the original anhydrous A material. The particle size was determined using a Microtrac SRA150 and the mean was 15.4 μm. The material was suspended at a concentration of 10 mg/ml in 0.5% methylcellulose on the morning of the dog study.

3.2.3. Determination of plasma concentrations

An analytical method using liquid chromatography/atmospheric pressure chemical ionization tandem mass spectrometry (LC/APCI-MS/MS) for the quantitation of **1** in dog plasma was developed and validated. The method employed a solid phase extraction (SPE) procedure to isolate **1** from the biological matrix. Both the liquid transfer and SPE process using 96-well plates were performed with a TECAN automatic liquid handling system. An analog of **1** was used as the internal standard. Reconstituted extracts were analyzed by LC/APCI-MS/MS in the selected reaction monitoring (SRM) mode. Chromatography was performed on a Kromasil C18 column (150 mm × 4.6 mm, 5 μm) using 90:10 acetonitrile:aqueous 0.1% trifluoroacetic acid. Under these conditions, no interference was observed for either **1** or its analog from the endogenous components of dog plasma. The assay had a lower limit of quantitation (LOQ) of 5 ng/ml plasma for **1** based on 0.1 ml aliquots of dog plasma. The standard curve was linear from 5 ng/ml to 20,000 ng/ml. The analysis time was 3.5 min per sample.

3.2.4. Data analysis

Area under the plasma concentration versus time curve (AUC) was calculated from observed data points by the linear trapezoidal rule with WinNonLin v.3.1 (Pharsight Corporation). The maximum plasma concentration (C_{max}) and time of C_{max} (T_{max}) were observed points. Arithmetic mean and standard error of the mean of AUC, C_{max}, and T_{max} were also calculated with WinNonLin. Treatments were compared using ANOVA and AUC and C_{max} values were log-transformed to normalize the distribution of the parameters.

3.3. Caco-2 cell culture

Cells were grown on Transwell polycarbonate membranes (3.0 μm pore size, 4.71 cm^2 surface area) for 21–28 days using previously described methods (Hidalgo et al., 1989). Mannitol flux was used as a measure of monolayer integrity. Transport studies were conducted in the apical (luminal) to basolateral (abluminal) direction using HBSS as the medium.

4. Results

4.1. Physicochemical characterization

Monohydrate A and monohydrate B were analyzed by TGA and showed a 3.9% weight loss between 50 and 125 °C indicative of a stoichiometric monohydrate (data not shown). DSC data showed a broad endotherm prior to the melting point of **1**, consistent with loss of water from the crystal lattice (data not shown). The crystal forms of **1** were distinguishable by XRPD, shown in Fig. 2. Following dosing, the crystal forms of the suspensions were verified by XRPD and all crystal forms were physically stable for the duration of the study.

Aqueous solubility was measured over 60 h for each of the three crystal forms and found to be approximately 0.007 mg/ml. Equilibrium solubility was obtained within 5 min and all forms gave similar solubility. The pH solubility profile showed a steep increase in solubility below a pH of 2.5 corresponding to a measured pK_a of 2.1 (data not shown).

Micrographs of the three crystal forms are shown in Fig. 3. The anhydrous A form had needle-like morphology, however both hydrate forms consisted of plates. The surface areas and particle sizes for each crystal form tested are described in Table 1.

4.2. In vivo studies

A summary of the pharmacokinetic parameters after oral administration of **1** at doses of 1, 50 and 100 mg/kg is shown in Table 2. The plasma concentration versus time curves for the 50 mg/kg dose are illustrated in Fig. 4. A three period crossover study was conducted initially to determine the effect of crystal form on the absorption of **1**. The batches of **1** used in these studies are noted with an asterisk in Table 2. The

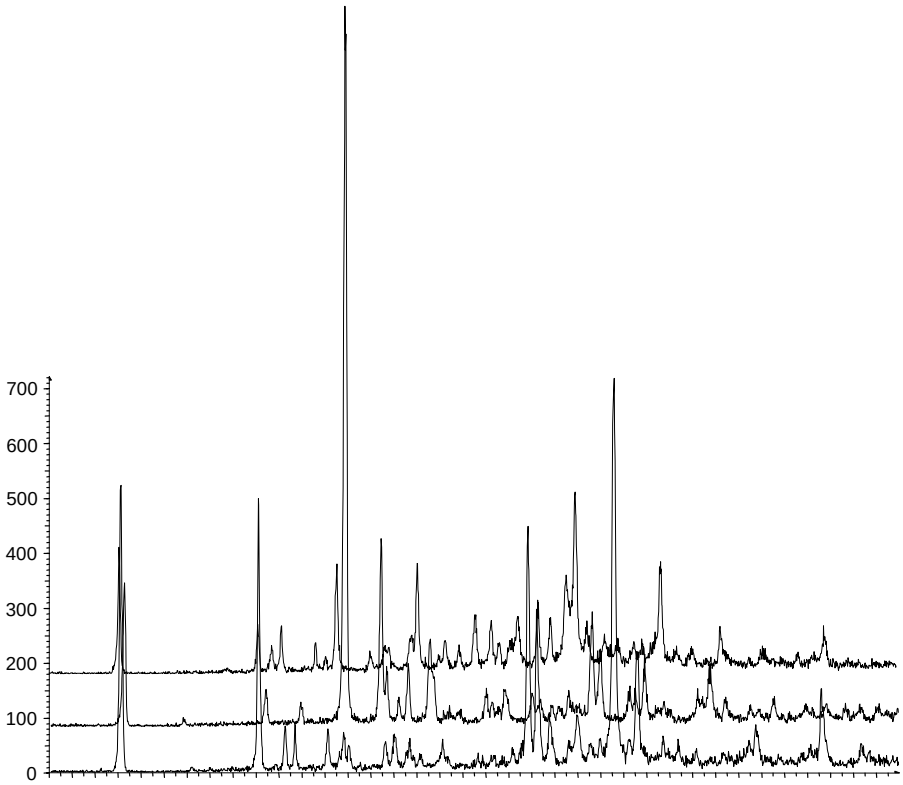

Fig. 2. Powder X-ray diffraction pattern of the TI monohydrate B (top), anhydrous A (middle) and monohydrate A (bottom) crystalline forms.

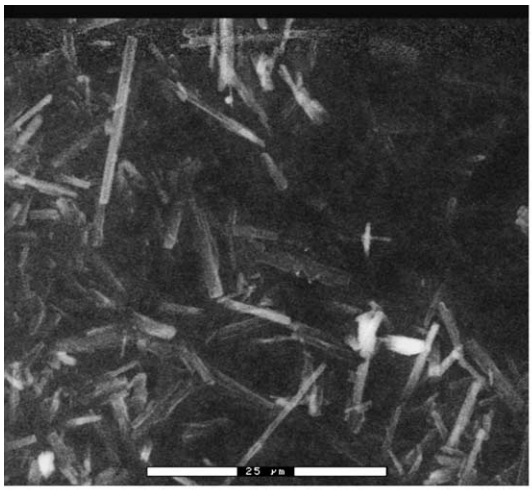

Anhydrous A

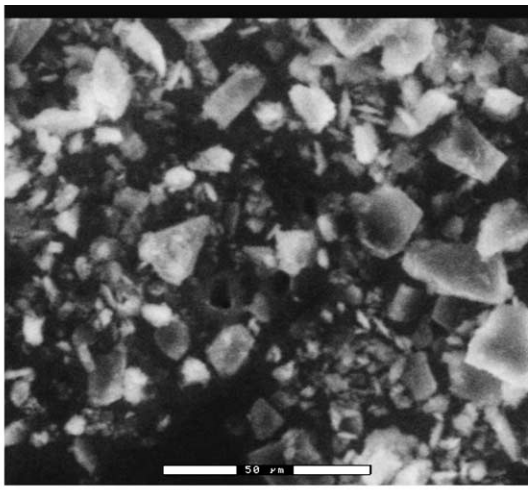

Monohydrate A

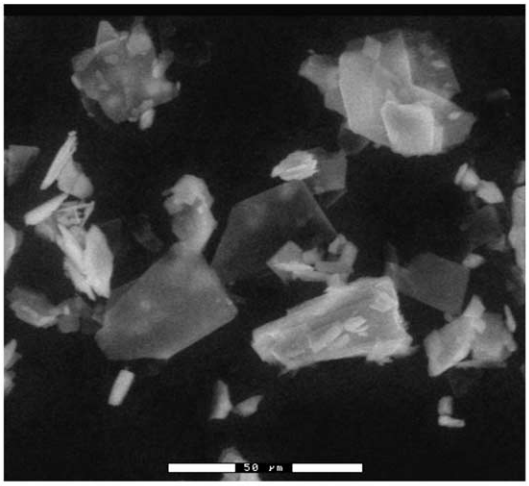

Monohydrate B

Fig. 3. Micrographs of the TI crystalline forms, illustrating the particle morphologies.

Table 1
Surface area and particle size of TI crystalline forms

	Anh A	Mono A	Anh A	Anh A	Mono A	Mono B	Mono A
Surface area (m^2/g)	6.9	6.1	5.2	4.5	2.3	1.7	1.2
Particle size							
Average (μm)	10	3.2	25	60	10	15	50
Range (μm)	5–25		5–105	5–200	5–90	4–45	5–170
<95% (μm)	15	5.8	40	100	15	25	70
PS reduction method	Sonication	Jet mill	Pin mill	None	Mortar/pestle	Pin mill	None
Morphology	Needles	Plates	Needles	Needles	Plates	Plates	Plates

Table 2
Summary of thrombin inhibitor pharmacokinetic parameters from Beagle dogs after oral administration of suspensions or a solution

Form	Dose (mg/kg)	Surface area (m^2/g)	$AUC_{0-2\,h}$ (μM h)	C_{max} (μM)	T_{max} (h)
Anhydrous A ($n = 5$)[a]	50	6.9	110.38 ± 8.55	15.61 ± 1.43	2.2 ± 0.4
Jet-milled monohydrate A ($n = 5$)	50	6.1	91.01 ± 11.12	14.16 ± 1.27	1.6 ± 0.2
Anhydrous A ($n = 5$)	50	4.5	92.55 ± 9.97	14.31 ± 1.55	2.0 ± 0.3
Monohydrate A ($n = 5$)[a]	50	2.3	50.46 ± 8.39	7.90 ± 1.23	2.0 ± 0.4
Monohydrate B ($n = 5$)[a]	50	1.7	39.36 ± 9.73	5.79 ± 1.27	1.5 ± 0.4
Monohydrate A ($n = 3$)	50	1.2	27.18 ± 6.18	4.27 ± 0.99	2.3 ± 0.3
Anhydrous A ($n = 3$)	100	5.2	108.64 ± 4.57	17.64 ± 1.65	2.7 ± 0.7
Solution ($n = 2$)	50	N/A	558.67 (545.78, 571.87)	98.37 (98.94, 97.80)	2.0 (2.0, 2.0)
Jet-milled monohydrate A ($n = 2$)	1	6.1	13.90 (14.03, 13.77)	2.23 (2.34, 2.13)	2.0 (1.0, 3.0)
Monohydrate A ($n = 2$)	1	1.2	6.62 (5.79, 7.57)	0.92 (0.77, 1.11)	3.5 (4.0, 3.0)

The AUC and C_{max} values are geometric mean ± S.E.M., T_{max} values are arithmetic mean ± S.E.M. *Note*. Individual values for groups with $n = 2$ are given in parentheses.
[a] Used in the initial three period crossover studies.

AUC and C_{max} values for the anhydrous A suspension were significantly higher than both monohydrate forms ($P < 0.05$) because the anhydrous A particles had a needle-like morphology leading to a higher surface area for the anhydrous A form. There were no significant differences observed between monohydrate A and monohydrate B where the morphologies and surface areas were similar. Additional studies were then conducted with larger particle size material of anhydrous A and monohydrate A as well as jet-milled monohydrate A to determine the contribution of surface area on the absorption of **1** at 50 mg/kg. The results are summarized in Table 2 and Fig. 4. There was a clear dependence of absorption on the surface area of the suspension particles as shown in Fig. 5 where graphs of 1/surface area versus 1/AUC and $1/C_{max}$ were linear with regression coefficients of 0.99.

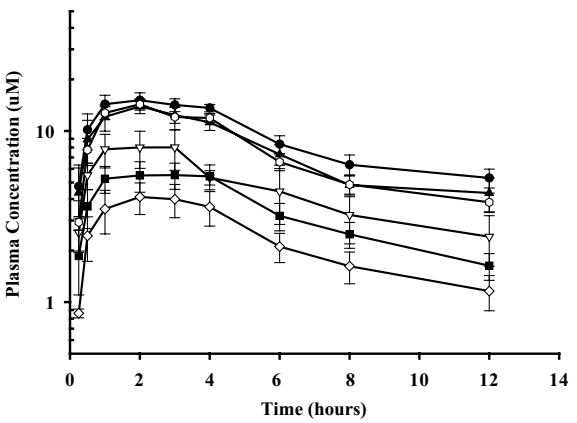

Fig. 4. Plasma concentration vs. time curves of monohydrate A, s.a. 1.2 m^2/g (◇), monohydrate B, s.a. 1.7 m^2/g (■), monohydrate A, s.a. 2.3 m^2/g (▽), anhydrous A, s.a. 4.5 m^2/g (▲), jet-milled monohydrate A, s.a. 6.1 m^2/g (⬡) and anhydrous A, s.a. 6.9 m^2/g (●) after oral administration to male Beagle dogs, 50 mg/kg ($n = 5$; mean ± S.E.).

Monohydrate A was also administered at a lower dose of 1 mg/kg and surface area effects were smaller at this dose. There was no increase in the exposure of TI when the dose was doubled to 100 mg/kg using an anhydrous A batch with slightly higher surface area than the anhydrous A at 50 mg/kg. The administration of a solution increased the absorption of TI approximately five-fold compared to the highest value obtained with a suspension. The solution achieved an AUC value of 559 μM h and a C_{max} of 98 μM.

Due to the surface area dependence on the oral absorption of **1**, two particle size reduction technologies were investigated. A colloidal dispersion was prepared by wet milling **1** using the NanoMill® milling system with HPC-SL and SLS as stabilizers. Additionally, the particle size of **1** was optimized using the SCF technology at Nektar. The exposure of the **1** colloidal dispersion and the SCF material were compared at 50 mg/kg in male Beagle dogs. The results of this study are shown in Table 3. Both the colloidal dispersion and the SCF material gave exposures in dogs that were greater than the suspension with a surface area of 6.1 m^2/g but less than the values of the solution. Also, the colloidal dispersion formulation appeared to perform slightly better than the SCF material suspension although the differences were not statistically significant ($P < 0.05$).

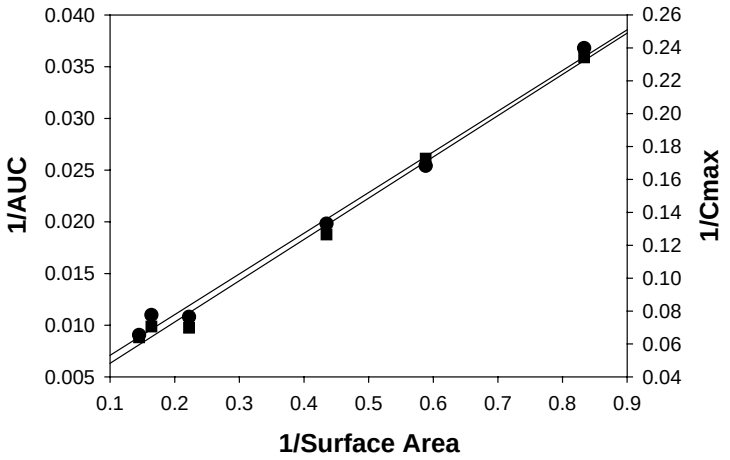

Fig. 5. 1/Surface area vs. 1/AUC (●) and $1/C_{max}$ (■) values using 50 mg/kg data.

Table 3
Summary of mean pharmacokinetic parameters from male Beagle dogs after administration of colloidal dispersion or SCF suspension at 50 mg/kg (mean ± S.D.)

Formulation	Surface area (m^2/g)	$AUC_{0-12\,h}$ (μM h)	C_{max} (μM)	T_{max} (h)
SCF material	35	161.71 ± 48.50	23.99 ± 7.87	3.3 ± 1.2
Colloidal dispersion	Not determined	230.86 ± 27.29	32.74 ± 6.07	3.0 ± 1.2

The plasma concentration versus time curves for the regional absorption studies with **1** are shown in Fig. 6. Pharmacokinetic parameters are summarized in Table 4. Systemic exposure (AUC) of **1** from a suspension delivered into the colon of dogs was approximately 60% of the AUC values from a solution formulation.

4.3. Caco-2 cell culture

The in vivo study results suggested that the absorption of **1** was dependent on the rate of dissolution of the compound. The high absorption observed after colonic administration provided further evidence that the permeability of **1** was not the limiting factor for absorption. To confirm these results, transport studies were conducted with Caco-2 cells. The apparent permeability of the thrombin inhibitor across Caco-2 cells in the apical to basolateral direction was 2.35E−05 ± 8.33E−07 cm/s. The apical to basolateral permeability of a model high permeability marker, caffeine, was 1.87E−05 ± 1.27E−06 cm/s, therefore **1** was classified as a highly permeable compound.

Table 4
Summary of thrombin inhibitor pharmacokinetic parameters from male triport Beagle dogs dosed at 1 mg/kg

Route	Formulation	Surface area	$AUC_{0-24\,h}$ (μM h)	C_{max} (μM)	T_{max} (h)
Oral	Solution in 50% HPβCD	N/A	24.28 ± 2.59	3.25 ± 0.24	1.3 ± 0.3
Jejunal	Solution in 50% HPβCD	N/A	21.62 ± 3.32	2.88 ± 0.42	1.5 ± 0.3
Colonic	Solution in 50% HPβCD	N/A	15.25 ± 4.89	1.22 ± 0.19	4.7 ± 0.7
Oral	Suspension in methocel	Mono A 6.1 m^2/g	17.27 (16.92, 17.61)	2.23 (2.34, 2.13)	2.0 (1.0, 3.0)
Colonic	Suspension in HPC-SL	Anhydrous A 4.5 m^2/g	9.52 ± 2.79	0.90 ± 0.23	4.7 ± 1.8

AUC and C_{max} values are geometric mean ± S.E. T_{max} values are arithmetic mean ± S.E.

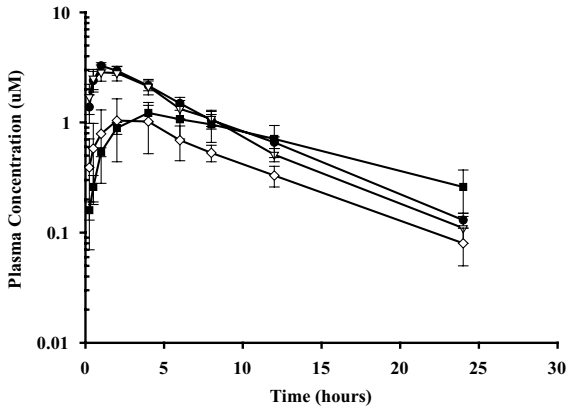

Fig. 6. Plasma concentration vs. time curves of TI following oral (●), jejunal (▽) and colonic (■) administration of a solution in 50% hydroxypropyl-β-cyclodextrin at a dose of 1 mg/kg ($n = 4$; mean ± S.E.) in Beagle dogs. The plasma concentration vs. time curve (◇) is also shown for the colonic administration of a TI suspension in 1.25% hydroxypropylcellulose at a dose of 1 mg/kg ($n = 3$; mean ± S.E.).

5. Discussion

It is well known and has been documented extensively that there are effects of polymorphism on absorption. Higuchi et al. (1963) and Shefter and Higuchi (1963) demonstrated that the thermodynamic properties of polymorphs and solvates will result in differences in their solubilities and dissolution rates, which can potentially lead to differences in their absorption properties. The anhydrous form of a compound will usually have a dissolution rate that exceeds the dissolution of the hydrates, however there have been exceptions to this rule (Brittain and Grant, 1999; Khankari and Grant, 1995; Nerurkar et al., 2000). Therefore, in situations where the absorption rate of a compound depends upon the rate of dissolution, both dissolution and absorption characteristics of the anhydrous and hydrate forms should be investigated.

In the first set of in vivo studies, the absorption of the anhydrous form of **1** was greater than the hydrate forms. In addition to the faster dissolution rate from the anhydrous form, the surface area was much higher than either of the hydrates due to its needle-like morphology. In subsequent studies with varying surface area and particle sizes, it was concluded that the absorption of TI was dependent on the surface area of the particles administered as suspensions and independent of the crystal forms. As illustrated in Fig. 5, there was a linear dependence of AUC and C_{max} values on surface area. If the surface area is extrapolated to infinity, this should approximate the values obtained with a solution. However, the actual values obtained with a solution were greater than the extrapolated values illustrating the complexity of the absorption process.

Two newer particle size reduction technologies were also investigated to demonstrate whether absorption could be further enhanced by decreasing the particle size of the drug to a greater extent than particle sizes obtained with conventional milling methods. A colloidal dispersion and a material which utilized supercritical fluid crystallization techniques were investigated. Both the colloidal dispersion and the SCF material gave exposures in dogs that were greater than the anhydrous form in suspension (SA 6.1 m^2/g) but less than the values of the solution. The values obtained with the SCF material were close to the extrapolated values of 233 μM h (AUC) and 33 μM (C_{max}) using Fig. 4 and the measured surface area of 35 m^2/g. Surface area was not measured for the colloidal dispersion. Although the AUC and C_{max} values obtained with the colloidal dispersion and the SCF material were not statistically different from each other, there was a trend for increased absorption with the colloidal dispersion formulation. This was likely due to the addition of particle size stabilizers into the dispersion during the milling process whereas the SCF material was simply suspended in methylcellulose.

Because of the various disadvantages of the current therapies for DVT, it would be ideal to obtain a therapeutic agent that produces a flatter profile and shows a decreased toxicity at higher does levels. The regional absorption study results indicated that **1** could be amenable to formulation as a controlled release product since **1** was reasonably absorbed along the gastrointestinal tract. The colonic AUC values were approximately 60% of the values obtained after oral dosing. According to the literature, the total gastrointestinal transit time for a conventional controlled release formulation is approximately 24 h with 20 h of this residence period in the colon (Prior et al., 2003). Due to the low fluid environment of the colon and the reduced surface area for absorption, compounds with low solubility would be likely to have limited absorption capabilities in the colon. **1** demonstrated adequate absorption after colonic administration therefore

a conventional controlled release formulation, such as an erodible matrix, may be possible assuming that the regional absorption in man is similar to dog.

From the Caco-2 cell transport studies, it was determined that the permeability of **1** was high. In the in vivo studies, **1** absorption was highly dependent on dissolution. Based on the low aqueous solubility of the thrombin inhibitor it would be classified as a class 2 compound in the Biopharmaceutics Classification System. The absorption properties of the final product, either as an immediate release or a controlled release, may be varied by influencing its dissolution rate due to the particle size of the bulk drug or the addition of excipients such as surfactants into the formulation.

In summary, it was evident in these studies that there was a significant effect of surface area on the absorption. Therefore, the absorption characteristics of the final clinical formulation can be influenced by the particle size of the bulk. Alternatively, further reduction of particle size or the addition of wetting agents into the formulation could help to decrease the dose needed for pharmacological activity. Also, if it was desirable to flatten the plasma concentration profile to decrease toxicity caused by C_{max} or to increase the apparent half-life, this compound appears to be amenable to a controlled release formulation approach. Finally, a controlled release formulation could be designed to achieve an optimal plasma concentration profile for therapy since the dissolution rate is the determining step for the absorption of **1**.

References

Brittain, H.G., Grant, D.J.W., 1999. Effects of polymorphism and solid-state solvation on solubility and dissolution rate. In: Brittain, H.G. (Ed.), Polymorphism in Pharmaceutical Solids, vol. 95. Marcel Dekker, Inc., New York, pp. 279–327.

Burgey, C., Robinson, K., Lyle, T., Sanderson, P., Lewis, S., Lucas, B., Krueger, J., Singh, R., Miller-Stein, C., White, R., Wong, B., Lyle, E., Williams, P., Coburn, C., Dorsey, B., Barrow, J., Stranieri, M., Holahan, M., Sitko, G., Cook, J., McMasters, D., McDonough, C., Sanders, W., Wallace, A., Clayton, F., Bohn, D., Leonard, Y., Detwiler, T., Lynch, J., Yan, Y., Chen, Z., Kuo, L., Gardell, S., Shafer, J., Vacca, J., 2003. Metabolism directed optimization of 2-aminopyrazinone acetamide thrombin inhibitors. Development of an orally bioavailable series containing P1 and P3 pyridines. J. Med. Chem. 46, 461–473.

Edwards, A., Shekunov, B., Kordikowski, A., Forbes, R., York, P., 2001. Crystallization of pure anhydrous polymorphs of carbamazepine by solution enhanced dispersion with supercritical fluids (SEDS^{TM}). J. Pharm. Sci. 90, 1115–1124.

Gustafsson, D., Nystrom, J.-E., Carlsson, S., Bredberg, U., Eriksson, U., Gyzander, E., Elg, M., Antonsson, T., Hoffmann, K.-J., Ungell, A.-L., Sorensen, H., Nagard, S., Abrahamsson, A., Bylund, R., 2001. The direct thrombin inhibitor megalatran and its oral prodrug H 376/95: intestinal absorption properties, biochemical and pharmacodynamic effects. Thrombosis Res. 2001, 171–181.

Hidalgo, I.J., Raubt, T.J., Borchardt, R.T., 1989. Characterization of the human colon carcinoma cell line (Caco-2) as a model system for intestinal epithelial permeability. Gastroenterology 96, 736–749.

Higuchi, W.I., Lau, P.K., Higuchi, T., Shell, J.W., 1963. Polymorphism and drug availability. J. Pharm. Sci. 52, 150–153.

Khankari, R.K., Grant, D.J.W., 1995. Pharmaceutical hydrates. Thermochim. Acta 248, 61–79.

Merisko-Liversidge, E., Liversidge, G.G., Cooper, E.R., 2003. Nanosizing: a formulation approach for poorly-water-soluble compounds. Eur. J. Pharm. Sci. 18, 113–120.

Nerurkar, M., Duddu, S., Grant, D.J.W., Rytting, J.H., 2000. Properties of solids that affect transport. In: Amidon, G.L., Lee, P.I., Topp, E.M. (Eds.), Transport Processes in Pharmaceutical Systems, vol. 102. Marcel Dekker, Inc., New York, pp. 575–610.

Prior, D.V., Wilding, I.R., Davis, S.S., 2003. HAD studies in life-cycle management. Pharm. Visions, Spring, 26–34.

Shefter, E., Higuchi, T., 1963. Dissolution behavior of crystalline solvated and nonsolvated forms of some pharmaceuticals. J. Pharm. Sci. 52, 781–791.

Palakodaty, S., York, P., 1999. Phase behavioral effects on particle formation processes using supercritical fluids. Pharm. Res. 16, 976–985.

Wahlander, K., Lapidus, L., Olsson, C.-G., Thuresson, A., Eriksson, U.G., Larson, G., Eriksson, H., 2002. Pharmacokinetics pharmacodynamics and clinical effects of the oral direct thrombin inhibitor ximelagatran in acute treatment of patients with pulmonary embolism and deep vein thrombosis. Thrombosis Res. 107, 93–99.